1997

Aspartate 19 and Glutamate 121 Are Critical for Transport Function of the myo-Inositol/H+ symporter from Leishmania donovani

Andreas Seyfang

Michael Kavanaugh
University of Montana - Missoula

Scott M. Landfear

THE JOURNAL OF BIOLOGICAL CHEMISTRY
Vol. 272, No. 39, Issue of September 26, pp. 24210–24215, 1997

Printed in U.S.A.

Aspartate 19 and Glutamate 121 Are Critical for Transport Function of the *myo*-Inositol/H^+ Symporter from *Leishmania donovani**

(Received for publication, April 16, 1997, and in revised form, July 16, 1997)

Andreas Seyfang‡§, Michael P. Kavanaugh¶, and Scott M. Landfear‡‖

From the ‡Department of Molecular Microbiology and Immunology and the ¶Vollum Institute, Oregon Health Sciences University, Portland, Oregon 97201

The protozoan flagellate *Leishmania donovani* has an active *myo*-inositol/proton symporter (MIT), which is driven by a proton gradient across the parasite membrane. We have used site-directed mutagenesis in combination with functional expression of transporter mutants in *Xenopus* oocytes and overexpression in *Leishmania* transfectants to investigate the significance of acidic transmembrane residues for proton relay and inositol transport. MIT has only three charged amino acids within predicted transmembrane domains. Two of these residues, Asp^{19} (TM1) and Glu^{121} (TM4), appeared to be critical for transport function of MIT, with a reduction of inositol transport to about 2% of wild-type activity when mutated to the uncharged amides D19N or E121Q and 20% (D19E) or 4% (E121D) of wild-type activity for the conservative mutations that retained the charge. Immunofluorescence microscopy of oocyte cryosections showed that MIT mutants were expressed on the oocyte surface at a similar level as MIT wild type, confirming that these mutations affect transport function and do not prevent trafficking of the transporter to the plasma membrane. The proton uncouplers carbonylcyanide-4-(trifluoromethoxy)phenylhydrazone and dinitrophenol inhibited inositol transport by 50–70% in the wild-type as well as in E121Q, despite its reduced transport activity. The mutant D19N, however, was stimulated about 4-fold by either protonophore and 2-fold by cyanide or increase of pH 7.5 to 8.5 but inhibited at pH 6.5. The conservative mutant D19E, in contrast, showed an inhibition profile similar to MIT wild type. We conclude that Asp^{19} and Glu^{121} are critical for *myo*-inositol transport, while the negatively charged carboxylate at Asp^{19} may be important for proton coupling of MIT.

In kinetoplastid protozoa such as *Leishmania* *myo*-inositol plays an especially important role as the precursor for various inositol phospholipids found in the great majority of surface molecules in these parasites. These include glycosyl-phosphatidylinositol-anchored surface proteins such as the major surface glycoprotein, gp63 (1, 2), or abundant inositol-containing glycolipids such as lipophosphoglycan (3) and glycoinositolphospholipids (4). Several of these surface molecules are involved in the invasion of macrophages in the mammalian host or the attachment of the parasite to the epithelium of the insect midgut. Strikingly, these glycosyl-phosphatidylinositol-anchored surface proteins and glycosyl-phosphatidylinositol-related glycolipids are several orders of magnitude more abundant on the surface of these parasites than in the mammalian host (5).

In a previous study (6), we cloned a *myo*-inositol transporter (MIT)[1] from the parasitic protozoan *Leishmania donovani*, the causative agent of fatal visceral leishmaniasis and an increasing health problem as an opportunistic infection in immunocompromised individuals (7, 8). MIT shows significant amino acid similarity with two inositol transporters from the yeast *Saccharomyces cerevisiae*, ITR1 and ITR2 (9), and is a member of the 12-transmembrane domain sugar transporter superfamily (10, 11). Functional expression of MIT in *Xenopus laevis* oocytes has revealed that it is an active *myo*-inositol/proton symporter driven by a proton gradient across the cell membrane (12). Subsequently, voltage clamp recording was used to characterize a 1:1 stoichiometry of transport with an ordered binding of a proton followed by a molecule of *myo*-inositol and subsequent transport of both molecules across the membrane (13). Finally, immunolocalization studies revealed that this transporter is expressed on the plasma membrane, flagellar pocket, and flagellum of the parasite (12).

Many transport processes in these flagellates are thought to be proton-driven, and MIT thus presents an excellent model for the study of one such proton symporter in *Leishmania*. A plasma-membrane proton ATPase has been identified in *L. donovani* (14), which can provide the transmembrane proton gradient for active secondary transporters. Knowledge of the function of protozoan transporters is still very limited, but from studies in prokaryotes, proton relay across cell membranes is thought to involve negatively charged amino acids within membrane-spanning domains (15). Two well studied examples are the lactose/H^+ symporter *lac* permease of *Escherichia coli* (16) and bacteriorhodopsin of halobacteria (17). Extensive mutagenesis of *lac* permease has revealed only four amino acids essential for transport, and all are thought to be charged transmembrane residues (18). In addition, studies with the melibiose permease from *E. coli* (19) have defined a role for transmembrane aspartate residues in interaction with the counterions H^+ or Na^+.

We chose the *Leishmania* *myo*-inositol/proton symporter

* This work was supported in part by National Institutes of Health (NIH) Grant AI25920 and Research Career Development Award AI01162 (to S. M. L.) and NIH Grant GM48709 (to M. P. K.). The costs of publication of this article were defrayed in part by the payment of page charges. This article must therefore be hereby marked "*advertisement*" in accordance with 18 U.S.C. Section 1734 solely to indicate this fact.

§ Supported by an Alexander von Humboldt Fellowship.

‖ To whom correspondence and reprint requests should be addressed: Dept. of Molecular Microbiology and Immunology, Oregon Health Sciences University, Mail code L-220, Portland, OR 97201-3098. Tel.: 503-494-2426; Fax: 503-494-6862; E-mail: landfear@ohsu.edu.

[1] The abbreviations used are: MIT, *myo*-inositol transporter from *Leishmania*; TM, transmembrane domain; ITR, inositol transporter from *S. cerevisiae*; AraE, arabinose transporter from *E. coli*; GalP, galactose transporter from *E. coli*; XylE, xylose transporter from *E. coli*; GLUT1, mammalian glucose transporter 1; FCCP, carbonylcyanide-4-(trifluoromethoxy)phenylhydrazone; PBS, phosphate-buffered saline; BSA, bovine serum albumin.

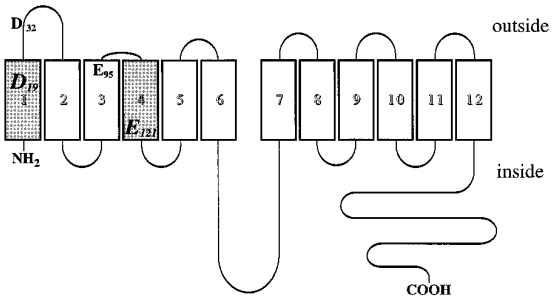

FIG. 1. **Secondary structure model of MIT.** *Boxed areas* indicate the 12 putative hydrophobic transmembrane domains, based on hydropathy analysis of the amino acid sequence (6, 42). *Single-letter code* is used to denote the acidic amino acids altered by site-directed mutagenesis. In *italics* are two amino acids that are critical for transport function of MIT as revealed from the functional expression of the mutants in this study. Asp^{19} and Glu^{121} are located within putative transmembrane domains (*shaded boxed areas*), which are potential candidates for mapping the substrate permeation pathway of MIT.

MIT as a model system for active transporters in lower eukaryotes. Examination of the MIT sequence revealed that this protein has only three charged amino acids within predicted transmembrane domains: aspartate 19, glutamate 95, and glutamate 121 (Fig. 1). In this study, we have used site-directed mutagenesis, in combination with functional expression of MIT mutants in *X. laevis* oocytes and overexpression in *L. donovani*, to investigate the significance of these acidic transmembrane residues in MIT for inositol uptake.

MATERIALS AND METHODS

Parasite Culture and MIT Expression in Oocytes—Promastigotes of the *L. donovani* DI-700 clone (Sudan strain 1S; Ref. 20) were cultured at 27 °C in Dulbecco's modified Eagle's medium, adapted for *Leishmania* (DME-L medium; Ref. 21), containing 0.3% bovine serum albumin (fraction V; Sigma) to replace fetal calf serum. Defolliculated stage V–VI *X. laevis* oocytes were microinjected with 8–10 ng (40 nl) of capped MIT cRNA, which was transcribed *in vitro* from linear MIT.pL2–5 template DNA by T7 RNA polymerase (Promega) as described previously (22). Injected oocytes were incubated for 3–5 days at 16 °C and 80 rpm shaking in ND-96 buffer (22) supplemented with 2.5 mM sodium pyruvate, 0.5 mM theophylline, and 50 μg/ml gentamycin.

Site-directed Mutagenesis—Oligonucleotide-directed, site-specific *in vitro* mutagenesis (23) was a modification of the procedure of Titus (24). Single-stranded DNA mutagenesis template was prepared from MIT.pL2–5 plasmid as described (25). Briefly, 0.06 pmol of single-stranded DNA mutagenesis template was annealed with 1.7 pmol of phosphorylated mutagenic oligonucleotide (Table I) for 5 min at 75 °C, gradually cooled down to 45 °C within 30 min and to room temperature within 10 min. Mutant strand synthesis by primer extension and ligation was carried out for 90 min at 37 °C using 8 units of T4 DNA polymerase (Promega) and 3 units of T4 DNA ligase (Promega). One-tenth of this mutagenesis reaction (about 10 ng of template DNA) was transformed into the *E. coli* ES1301 *mut S* strain to suppress *in vivo* mismatch repair (26) and amplified in liquid culture under ampicillin selection. Subsequently, 1 ng of *mut S*-derived plasmid DNA was transformed into *E. coli* XL-1 Blue cells and individual colonies were selected from agar plates. Mutagenic oligonucleotides were designed to generate the appropriate aspartate or glutamate mutation and to introduce simultaneously a silent restriction endonuclease site alteration (Table I). Mutant clones were identified by restriction enzyme mapping with a yield of 20–50% of mutants. The presence of the mutation was later verified by DNA sequencing using the dideoxy chain termination method (27). For the mutations affecting inositol uptake (D19N, D19E, E121Q, E121D), the entire mutant gene was sequenced to confirm the introduction of the desired mutation and the absence of any other sequence alterations.

Plasmid Constructs and Transfection into Leishmania—For expression of the MIT gene in oocytes, MIT (formerly designated D1; Ref. 6) was subcloned into the *Xenopus* expression vector pL2–5 (Ref. 28; kindly provided by Dr. Susan Amara, Vollum Institute) as reported by Drew *et al.* (12) to produce the MIT.pL2–5 plasmid. For overexpression of the MIT gene in *L. donovani* promastigotes, the MIT *Hin*dIII-*Hin*dIII insert of MIT.pL2–5 was subcloned into the *Leishmania* expression vector pX-H, derived from vector pX (Ref. 29; kindly provided by Dr. Stephen Beverley, Harvard Medical School) by introducing a *Hin*dIII site into the *Bam*HI site of pX, to produce the MIT.pX-H plasmid. Transfection of the MIT.pX-H plasmid into *L. donovani* promastigotes was performed by electroporation as described previously (30), and transfectants were selected in liquid medium containing 200 μg/ml neomycin analog G418 (Life Technologies, Inc.).

Transport Assays—For transport assays in *Leishmania* and oocytes, *myo*-[2-^{3}H]inositol (specific activity of 21 Ci/mmol; NEN Life Science Products) was utilized. Promastigotes from middle to late log phase *L. donovani* culture, transfected with MIT.pX-H, were washed twice in phosphate-buffered saline (PBS, pH 7.4) and resuspended in PBS. Transport was measured at 25 °C and initiated by adding 100 μl of cells (5×10^7) to 100 μl of radiolabeled *myo*-inositol at 50 μM final concentration in PBS. At various time points between 10 and 120 s, transport was stopped by spinning the cells through an oil cushion of 100 μl of dibutyl phthalate in a microcentrifuge tube, followed by immediate snap freezing of the tube in a dry ice/ethanol bath. The tip of the tube with the frozen cell pellet was then clipped off into 250 μl of 1% SDS, mixed with 2 ml of EcoLume (ICN, Costa Mesa, CA), and analyzed by liquid scintilation counting. The initial *myo*-inositol uptake rate was determined by linear regression analysis from the linear uptake range for the various transfectants.

Transport measurements in *Xenopus* oocytes were performed at room temperature and initiated by adding three or four oocytes to 300 μl of radiolabeled *myo*-inositol (50 μM to 3 mM final concentration) in ND-96 buffer. After 30 min of incubation, the oocytes were washed three times in 2 ml each of ND-96 buffer. Subsequently, each oocyte was individually solubilized in 250 μl of 1% SDS and analyzed by liquid scintilation counting in EcoLume as described above. Water-injected oocytes served as control for MIT-specific inositol uptake determination. For inhibitor studies, protonophores or other potential inhibitors (applied from an ethanol stock solution) were preincubated with the oocytes for 10 min prior to the initiation of uptake assays, and cells incubated with 1% ethanol served as control. Statistical analysis of the data was performed by the paired sample *t* test, and all *p* values are two-tailed (31). For the substrate saturation kinetics, K_m and V_{max} values were determined by least squares fit of the data to the Michaelis-Menten equation, employing the Levenberg-Marquardt algorithm (KaleidaGraph program, Synergy Software) (22).

Confocal Immunofluorescence Microscopy—Antibody against the 136-amino acid hydrophilic COOH-terminal domain of MIT (MIT-COOH) was produced against an MIT-COOH glutathione *S*-transferase fusion protein (12). For MIT immunolocalization in oocyte cryosections, MIT-expressing oocytes (four per wild-type or mutant) were fixed in 3% formaldehyde/PBS for 2 h at room temperature, infiltrated with 20% sucrose/PBS overnight at 4 °C, and embedded in Tissue-Tek O.C.T. compound (Sakura Finetek U.S.A., Torrance, CA) for at least 5 h at room temperature (32). Embedded samples were rapidly frozen in dry ice, and semithin cryosections (8–10 μm) were cut on a cryostat, mounted on poly-L-lysine-coated slides, dried, and stored at −20 °C. Subsequently, MIT protein was immunolocalized in oocyte sections blocked with 5% BSA in PBS for 10 min, followed by a 1-h incubation with MIT-COOH rabbit antiserum (diluted 1:100 in 1% BSA/PBS) and Texas Red-conjugated secondary antibody (Molecular Probes, Eugene, OR; diluted 1:500 in 1% BSA/PBS) for 30 min. Oocyte sections were examined with a Leica confocal laser-scanning microscope (Leica Lasertechnik GmbH, Heidelberg, Germany) with a Leitz × 63 oil immersion lens as described previously (30). All oocytes in Fig. 4 came from the same batch, and for each mutant, oocytes from the same microinjection were tested for mutant-specific inositol uptake prior to the embedding procedure.

RESULTS

Inositol Uptake in MIT Mutants—As shown in Fig. 2, alteration of either Asp^{19} (TM1) or Glu^{121} (TM4) from the charged carboxylate to the uncharged amide reduced transport activity to about 2% of wild-type activity when the mutants were expressed in *Xenopus* oocytes. For all measurements in oocytes, MIT-specific inositol uptake was determined by subtracting the values of water-injected control oocytes from the same batch for each experiment, and the resulting D19N-specific and E121Q-specific inositol uptake, although low, was significantly different from the background level of water-injected oocytes, with $p < 0.01$ and $p < 0.02$, respectively (paired sample *t* test). The mutant D32N in extracellular loop 1 served as control and did

TABLE I
Mutations introduced into MIT

Italics indicate nucleotides replaced in mutants. The affected codon is underlined. Colons indicate beginning and end of the affected restriction endonuclease recognition sequence with the cutting site marked by an asterisk. The mutagenic primer is in antisense orientation and was annealed to single-stranded template DNA of sense orientation. Nucleotide position is numbered in sense orientation according to Langford *et al.* (6).

MIT	Mutagenic primer	Nucleotide	Nucleotide change	Restriction site alteration
D19N	5′-GAT:GAC GC*C CGT GT*T*:ATA GCC GAA GAG-3′	730	G → A	*Drd*I site lost
D19E	5′-GAT:GAC GC*C CGT *TT*C:ATA GCC GAA GAG-3′	732	C → A	*Drd*I site lost
D32N	5′-GAA GCC:GAA GT*G GT*T*C:TT CAT CTG GAA-3′	769	G → A	New *Xmn*I site
E95Q	5′-CAC GAG CAC CAC TT:*G* CAC*ATT TGG G:GC-3′	958	G → C	*Bsi*YI site lost
E121Q	5′-CGG CGA TGT TAC TT:*G**CGC:CAG GTA CAC-3′	1036	G → C	New *Cfo*I site
E121D	5′-TGT TAC *GTC* CGC CAG GTA C:AC *A*G*G A:AT GGT GGC-3′	1023, 1038	A → T, A → C	*Bsr*I site lost

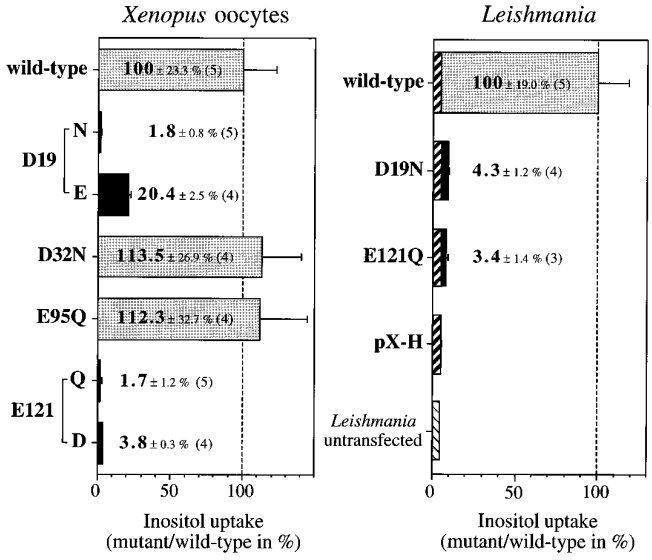

FIG. 2. ***myo*-Inositol uptake in MIT mutants expressed in *X. laevis* oocytes or overexpressed in *Leishmania* parasites.** For uptake studies in oocytes (*left*), *in vitro* transcribed cRNA was microinjected at a concentration of 8–10 ng/oocyte. After 3 days of expression, uptake of *myo*-[^{3}H]inositol was assayed at 50 μM substrate concentration for 30 min. Values represent means ± S.D. of four or five independent experiments (number in parenthesis) with three or four oocytes each, after subtracting the values for water-injected oocytes as control. Wild-type inositol uptake was 51.4 ± 11.7 pmol/30 min/oocyte. For uptake studies in *L. donovani* parasites (*right*), MIT wild type and mutants were subcloned into the *Leishmania* expression vector pX-H (containing *neo*^{r}) and transfected into promastigote cells. *myo*-[^{3}H] Inositol uptake is given as a percentage relative to wild-type activity (1526.7 ± 290.5 pmol/min/10^8 cells) after subtraction of endogenous inositol uptake (*cross-hatched area*) of control cells transfected with the vector (pX-H) alone. *Solid bars* in both *panels* indicate mutants for which inositol transport was significantly different ($p < 0.001$) from MIT wild type, analyzed by paired sample *t* test.

not affect inositol uptake significantly. One of the acidic transmembrane residues, Asp^{95} (TM3), also showed no effect when mutated (Fig. 2). Subsequent transfection and overexpression of MIT in *Leishmania* confirmed the significance of Asp^{19} and Glu^{121} for MIT transport function. Transport was reduced by 96 and 97%, respectively, in flagellates overexpressing the two mutants compared with MIT wild-type overexpressors (Fig. 2). MIT overexpressors showed 21-fold higher inositol uptake compared with endogenous MIT transport activity of *Leishmania* transfected with the vector alone, and inositol transport in D19N- and E121Q-overexpressing parasites was also significantly different from endogenous MIT transport ($p < 0.01$ and $p < 0.06$, respectively). Finally, growth of transfected parasites under drug selection did not affect MIT activity, with 72.4 ± 13.7 pmol/min and 70.7 ± 5.6 pmol/min per 10^8 cells in pX-H-transfected flagellates and untransfected *Leishmania*, respectively (Fig. 2).

As a next step, we mutated the two residues affecting inositol uptake to the alternative carboxylate form and thus retained the charge. These conservative mutations both showed a significant reduction on inositol uptake compared with MIT wild type, but inositol uptake was 11-fold higher in D19E and 2-fold higher in E121D than in the respective nonconservative mutations to the uncharged amide (Fig. 2). Thus, amino acid side chain length appears to be more restricted for the negative charge at position 121 than for the apparently more flexible negative charge at position 19.

Substrate saturation kinetics revealed that the transporter's substrate affinity was not significantly changed in the two mutants affecting inositol uptake, instead demonstrating a dramatic reduction of the V_{max} values by 97% (D19N) and 98% (E121Q) compared with MIT wild-type activity (Fig. 3 and Table II). Alternative monovalent cations such as Li^+ or Rb^+ at 1 mM concentration in the uptake buffer could not restore inositol transport activity in the two mutants with reduced inositol uptake (data not shown).

Immunolocalization of MIT Mutants on Oocyte Plasma Membrane—Immunofluorescence microscopy of oocyte cryosections showed that MIT mutants were expressed on the oocyte surface in similar quantity as MIT wild type (Fig. 4), confirming that these mutations affect transport function, inhibiting inositol uptake up to 98%, and do not prevent trafficking of the transporter to the plasma membrane. Water-injected oocytes served as control and did not show any plasma membrane staining (Fig. 4). MIT was expressed homogeneously over the entire oocyte plasma membrane of both animal and vegetal pole. The results shown in Fig. 4 were confirmed by examining four separate oocytes expressing each MIT mutant.

Effect of Proton Gradient Uncouplers and pH on Inositol Uptake by MIT Mutants—Subsequently, we investigated the effect of two protonophores and uncouplers on the various mutants. The proton gradient uncouplers FCCP and dinitrophenol inhibited inositol transport by 50–70% in the wild-type as well as in the control mutant D32N. The same protonophore sensitivity was found in the MIT mutants E95Q and E121Q, despite the reduced transport activity of the latter one (Fig. 5). Surprisingly, one mutant, D19N, completely lost all inhibition and instead was stimulated about 4-fold by either protonophore (statistical significance: $p < 0.002$, paired sample *t* test). Subsequently, we further investigated the pharmacology and pH dependence of this interesting Asp^{19} mutant (Table III). Phenol did not show the stimulatory effect on D19N and served as control for the *protonophore* effect of dinitrophenol, separating from its effects as an organic solvent. Monensin had no effect on inositol uptake in any of the Asp^{19} mutants or MIT wild type, and as a Na^+ ionophore it served as control for the H^+ specificity of the D19N effect (Table III, top). Finally, cyanide showed a similar effect as the protonophores and inhibited MIT wild type and the D19E mutant 44–50% but stimulated inositol uptake about 2-fold in the D19N mutant ($p < 0.02$). This latter reagent was used to indirectly reduce the proton gradient by affecting H^+-ATPase activity, due to the inhibition of cyto-

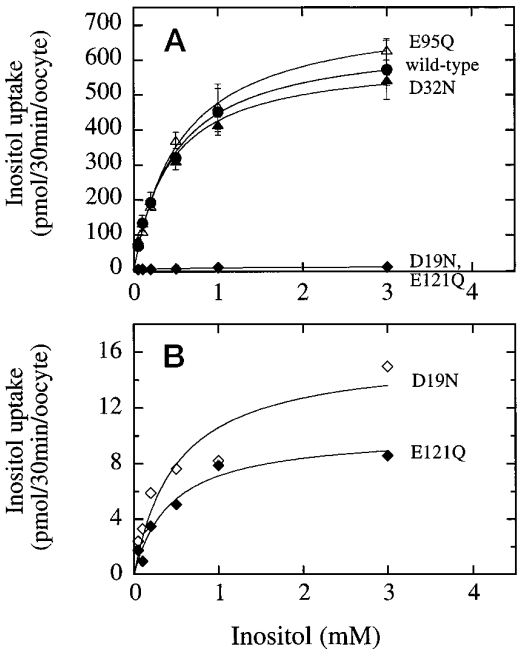

FIG. 3. **Concentration-dependent inositol uptake in MIT mutants.** *A*, substrate saturation kinetics were determined in MIT-expressing oocytes for a concentration range of 50 μM to 3 mM *myo*-inositol (mean ± S.D. of three or four independent experiments). For each data point, the average nonspecific inositol uptake by control water-injected oocytes was subtracted as described for Fig. 2. *B*, enlargement for the D19N and E121Q mutants with reduced inositol transport activity (a representative uptake curve of four or three independent experiments, respectively, is shown).

TABLE II
Kinetics of inositol uptake in MIT mutants

Substrate saturation kinetics of *myo*-inositol uptake were determined in *Xenopus* oocytes injected with 8–10 ng of *in vitro* transcribed cRNA. A substrate concentration range of 50 μM to 3 mM *myo*-inositol was used. The means ± S.D. from three or four independent experiments (number on the right), each performed with three or four oocytes, are shown. V_{mut}/V_{wt} was obtained by dividing each V_{max} value by the V_{max} determined for the wild-type transporter.

	K_m	V_{max}	V_{mut}/V_{wt}	n
	μM	*pmol/30 min/oocyte*	%	
Wild type	640 ± 144	465 ± 152	100	4
D19N	509 ± 229	16 ± 2.5	3.4 ± 0.5	4
D32N	554 ± 147	556 ± 136	120 ± 29	3
E95Q	699 ± 277	556 ± 166	120 ± 36	3
E121Q	437 ± 121	10 ± 1.0	2.2 ± 0.2	3

chrome activity and reduction of ATP levels in the cells.

A reversal of pH dependence of inositol uptake in the D19N mutant compared with MIT wild type and D19E (Table III, bottom) further supported the results obtained by the proton gradient uncouplers. Inositol uptake in the D19N mutant was stimulated about 1.7-fold when the extracellular proton concentration was reduced from pH 7.5 to pH 8.5, whereas MIT wild type was inhibited about 60% at pH 8.5. Conversely, an increased extracellular proton concentration at pH 6.5 stimulated inositol uptake in MIT wild type about 3.5-fold compared with pH 7.5, while D19N was inhibited about 10% (Table III, bottom). The cumulative data in Table III show that the conservative mutant D19E has the same inhibition profile as MIT wild type and, together with the other controls, suggest that the stimulatory effect of protonophores or reduced extracellular proton concentration upon D19N results from the removal of the charge of the carboxylate and a reduction of the cell's proton gradient. These results underscore the probable importance of aspartate 19 in proton symport, although we do not

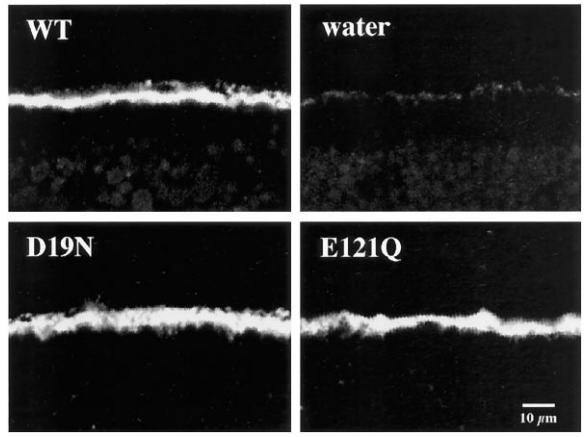

FIG. 4. **Confocal immunofluorescence micrographs of MIT-expressing oocytes.** Oocytes were injected with cRNA or water as control and assayed for inositol uptake as described for Fig. 2. For immunolocalization, oocytes from the same batch were fixed in 3% formaldehyde/PBS, infiltrated with 20% sucrose/PBS, and embedded in O.C.T. compound. Samples were rapidly frozen in dry ice, and semithin cryosections (8–10 μm thick) were cut for subsequent immunolocalization by anti-MIT polyclonal antibody, followed by Texas Red-conjugated secondary antibody and confocal microscopy analysis. A representative sector of an oocyte is shown in each *panel* containing the plasma membrane (immunostained against MIT proteins) and the unstained cytoplasm beneath. *WT*, wild-type.

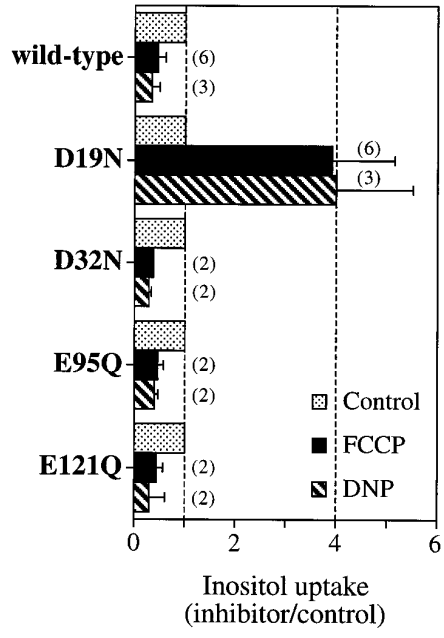

FIG. 5. **Effect of protonophores on inositol uptake.** *Xenopus* oocytes were injected with MIT cRNA and assayed for *myo*-inositol uptake in the presence of protonophore FCCP or dinitrophenol (*DNP*) or 1% ethanol as control. Water-injected oocytes with identical treatment served as control to determine MIT-specific inositol uptake. Inhibition data are expressed relative to the control for each mutant independently (mean ± S.D.). The number of independent experiments for each mutant, each performed with three or four oocytes, is given in *parentheses*.

currently understand how this stimulation occurs. One possibility is that alteration of the transporter's protonation may lead to conformational changes in the D19N mutant and the observed stimulatory effect on inositol transport.

DISCUSSION

Acidic amino acid residues have been shown to be important in translocation of protons across membranes in bacteriorhodopsin, where Asp[85] and Asp[96] have been postulated to play

TABLE III

Pharmacology and pH dependence of inositol uptake in MIT wild type and D19 mutants

Xenopus oocytes were injected with *in vitro* transcribed MIT cRNA and assayed for *myo*-inositol uptake in the presence of (top) various inhibitors or 1% ethanol as control, or (bottom) various pH values of the uptake medium. Water-injected oocytes served as control to determine MIT-specific inositol uptake. Data were obtained at 50 μM inositol concentration from three or six independent experiments (number in parentheses) with three or four oocytes each (mean ± S.D.); 100% inositol uptake equal to 51.4, 0.93, or 10.5 pmol/30 min/oocyte for MIT wild type, D19N, or D19E mutant, respectively. Statistical significance compared with wild-type: *, $p < 0.10$; **, $p < 0.02$; ***, $p < 0.002$ (paired sample t test).

	Inositol uptake		
	Wild-type	D19N	D19E
		% (inhibitor/control)	
Inhibitor			
Control, 1% ethanol (6)	100	100	100
FCCP, 10 μM (6)	45.7 ± 15.6	391.1 ± 124.9***	56.3 ± 9.9
DNP, 1.5 mM (3)	34.3 ± 15.5	399.9 ± 151.7*	41.6 ± 17.8
Phenol, 1.5 mM (3)	104.8 ± 15.6	88.2 ± 3.6	89.0 ± 18.6
Monensin, 2 μM (3)	98.7 ± 6.8	100.5 ± 9.2	108.0 ± 5.2
NaCN, 1 mM (3)	50.4 ± 15.3	212.2 ± 34.9**	56.0 ± 16.2
		% (pH/control)	
pH of uptake medium			
pH 6.5 (3)	345.9 ± 52.6	89.6 ± 4.3**	122.4 ± 18.1
pH 7.5, control (3)	100	100	100
pH 8.5 (3)	41.2 ± 3.5	174.5 ± 35.1**	74.7 ± 20.8

direct roles in transfer of protons from inside to outside of the membrane (17). In the *lac* permease, Asp^{325} and three positively charged residues, His^{322}, Arg^{302}, and Lys^{319}, have been proposed as important residues for transport (16). Furthermore, in the *E. coli* melibiose permease, the acidic transmembrane residues Asp^{31}, Asp^{51}, Asp^{55}, and Asp^{120} have been implicated in interaction with both the H^+ and Na^+ cosubstrates (19). Remarkably, alteration of these residues changes the counterion specificity of this transporter. The apparently central role of charged transmembrane residues in transporter function encouraged us to identify and alter, by mutagenesis, such residues in MIT. Indeed, we have found that alteration of two of the three charged transmembrane residues almost eliminates transport activity. Although we do not know the specific function of Asp^{19} or Glu^{121} in MIT, these amino acids are likely candidates to be directly involved in transport mechanism. Conversely, alteration of Glu^{95} to Gln does not affect transport function, indicating that alteration of any charged transmembrane residue is not sufficient to eliminate transport function.

Subsequently, we compared the conservation of the three acidic transmembrane residues in MIT with five inositol and sugar/proton symporters from bacteria and yeast (Fig. 6), all sharing an active transport mechanism. Amino acid sequence alignment of the corresponding transmembrane domains 1, 3, and 4 was analyzed and quantitated through the variability profile as the number of different amino acids occurring at each locus (33). Asp^{19} and Glu^{121} of MIT were 100% conserved in all six proton symporters, whereas Glu^{95} was not conserved, with three different amino acids found at that locus in the six transporters (Fig. 6). Conservation of amino acids is a sign of their potential significance with regard to protein function, and these findings match our mutagenesis studies and underscore the importance of Asp^{19} and Glu^{121} for MIT function. While the MIT Asp^{19} position is an aspartate in these six proton symporters, it is an asparagine in the homologous facilitated diffusion transporter GLUT1. Glu^{121}, however, remains a glutamate in GLUT1. The possible importance of Asp^{19} for proton binding is underscored by the pharmacology of MIT wild type and Asp^{19} mutants (Table III). Active proton-coupled inositol transport is found for a carboxylate side chain at residue 19 (Asp^{19} or Glu^{19}), as suggested by inhibition with protonophores or cyanide. The mutant with the uncharged amide Asn^{19}, in contrast, is not inhibited by proton uncouplers. Currently, we cannot fully explain the stimulatory effect of a reduced proton gradient upon the D19N mutant, other then a possible allosteric effect that may be caused by changes in the protonation of the transporter mutant. Alteration of transporter ionization was also suggested for the increased transport activity at acidic pH for a facilitated diffusion sugar transporter from lysosomes (34).

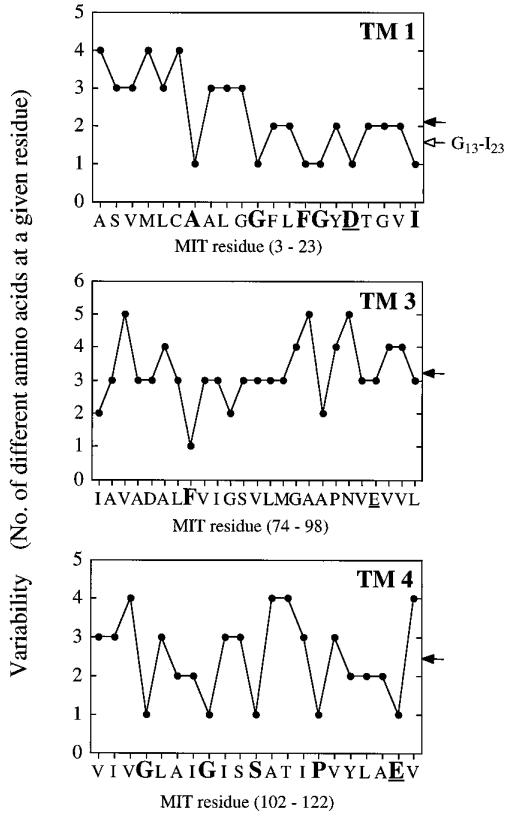

FIG. 6. **Variability profile of MIT transmembrane domains 1, 3, and 4 aligned with five proton symporters from bacteria and yeast.** Conservation at each site of the three transmembrane segments is quantitated through the variability profile as the number of different amino acids occurring at the locus (33). The plot is calculated from an amino acid sequence alignment of MIT with two inositol transporters from *S. cerevisiae*, ITR1 and ITR2, and three active sugar transporters from *E. coli*, AraE, GalP, and XylE (sequence alignment according to Refs. 11 and 12). Residues 100% conserved through all six proton symporters are *enlarged in boldface type*. Note a periodicity of three to four residues for this conservation pattern, suggestive of functionally conserved residues along one side of an α-helical structure. *Underlined* are residues Asp^{19}, Glu^{95}, and Glu^{121}, respectively. *Filled arrows* at the *right ordinate* mark the mean variability number for each transmembrane segment or MIT residues Gly^{13}–Ile^{23} in TM1 (*open arrow*).

Comparison of the three transmembrane domains 1, 3, and 4 in MIT, ITR1, ITR2, AraE, GalP, and XylE (Fig. 6) revealed a significantly higher degree of conservation in helices 1 and 4 with 66.2 and 62.0% amino acid identity, respectively, compared with helix 3 with 44.9% identity. In helix 1, identity among the six proton symporters increases to 84.9% for the carboxyl-terminal half of the transmembrane domain (MIT G13-I23), which contains residue Asp^{19}. Remarkable is a periodicity of three to four residues for the conservation pattern in helix 1 (Ala^9–Gly^{13}–Phe^{16}–Asp^{19}–Ile^{23}) and helix 4 (Gly^{105}–Gly^{109}–Ser^{112}–Pro^{116}), suggestive of α-helical character and orientation along a conserved and functionally important stretch of the transmembrane segment, potentially part of the substrate permeation pathway.

The *Leishmania* MIT is a member of the large sugar transporter superfamily, ranging from bacteria to plants and mammals, and this protozoan transporter serves as a model for active transporters in early eukaryotes. The bacterial disaccharide/cation symporters, lactose permease and melibiose permease, are usually grouped in a separate family, based on structural and functional data (35, 10, 11). For *lac* permease it was demonstrated that transmembrane domains 6–12 (designated C_6) are sufficient to catalyze facilitative transport (18), and four charged transmembrane residues essential for transport function are located in C_6. This is distinct from MIT, where charged residues important for function are in the NH_2-terminal half of the carrier. However, four aspartate residues in the NH_2-terminal half of the melibiose transporter are thought to be important for counterion binding (36), similar to the results obtained with MIT.

Site-directed mutagenesis in the small number of transporters extensively studied has revealed that residues critical for transport activity are rather rare, and in the mammalian glucose transporter GLUT1 only two residues (Gln^{161} and Trp^{412}) were found to greatly influence transport activity (37). These residues lie within transmembrane domains 5 and 11, respectively, and support the idea based on ligand binding and labeling studies that the C-terminal part of GLUT1 may form the aqueous pore for the substrate permeation pathway (11, 38). In MIT, however, transmembrane domains 1 and 4 appear to be important for substrate transport. The observation that either NH_2-terminal or C-terminal half of the various transporters are implicated to align the substrate translocation pathway may be explained by the symmetrical arrangement of two six-helix bundles, derived from an internal gene duplication event in an ancestral six-transmembrane domain transporter (35, 11), where one of the two six-helix bundles retains the substrate translocation pathway in the modern 12-helix transporter. However, this hypothesis has been challenged recently by a photoaffinity labeling study of GLUT1 (39) showing evidence that not only the carboxyl-terminal half but also the amino-terminal half of GLUT1 helices participates in the putative substrate channel formation.

In this study, we have shown the importance of two transmembrane carboxylate residues for transport function in a protozoan proton symporter, similar to results observed with active transporters from bacteria. These residues may play a direct role in the transport of protons, although this conjecture remains to be proven. For most transporters, the location of the "permeation pathway" is still largely unknown. It is likely that Asp^{19} and Glu^{121} are on this permeation pathway in MIT. The results presented here suggest experiments to test the possibility that Asp^{19} and Glu^{121} are on this transport pathway, including systematic chemical modification of residues on putative transmembrane helices 1 and 4, both in the presence and absence of *myo*-inositol (40, 41).

Acknowledgments—We thank Weibin Zhang for harvesting *Xenopus* oocytes and George Cole for cutting the cryosections. We thank all members of the Kavanaugh lab for helpful advice with handling and microinjection of the oocytes.

REFERENCES

1. Chang, C. S., and Chang, K.-P. (1986) *Proc. Natl. Acad. Sci. U. S. A.* **83,** 100–104
2. Russell, D. G., and Wilhelm, H. (1986) *J. Immunol.* **136,** 2613–2620
3. Turco, S. J., and Descoteaux, A. (1992) *Annu. Rev. Microbiol.* **46,** 65–94
4. McConville, M. J., and Ferguson, M. A. J. (1993) *Biochem. J.* **294,** 305–324
5. Ferguson, M. A. J., Brimacombe, J. S., Cottaz, S., Field, R. A., Güther, L. S., Homans, S. W., McConville, M. J., Mehlert, A., Milne, K. G., Ralton, J. E., Roy, Y. A., Schneider, P., and Zitzmann, N. (1994) *Parasitology* **108,** S45–S54
6. Langford, C. K., Ewbank, S. A., Hanson, S. S., Ullman, B., and Landfear, S. M. (1992) *Mol. Biochem. Parasitol.* **55,** 51–64
7. de Gorgolas, M., and Miles, M. A. (1994) *Nature* **372,** 734
8. Alvar, J. (1994) *Parasitol. Today* **10,** 160–163
9. Nikawa, J., Tsukagoshi, Y., and Yamashita, S. (1991) *J. Biol. Chem.* **266,** 11184–11191
10. Henderson, P. J. F. (1991) *Curr. Opin. Struct. Biol.* **1,** 590–601
11. Baldwin, S. A. (1993) *Biochim. Biophys. Acta* **1154,** 17–49
12. Drew, M. E., Langford, C. K., Klamo, E. M., Russell, D. G., Kavanaugh, M. P., and Landfear, S. M. (1995) *Mol. Cell. Biol.* **15,** 5508–5515
13. Klamo, E. M., Drew, M. E., Landfear, S. M., and Kavanaugh, M. P. (1996) *J. Biol. Chem.* **271,** 14937–14943
14. Zilberstein, D., and Dwyer, D. M. (1988) *Biochem. J.* **256,** 13–21
15. Nagle, J. F., and Morowitz, H. J. (1978) *Proc. Natl. Acad. Sci. U. S. A.* **75,** 298–302
16. Kaback, R. (1992) in *Molecular Biology of Receptors and Transporters: Bacterial and Glucose Transporters* (Friedlander, M., and Mueckler, M., eds) pp. 97–125, Academic Press, Inc., San Diego
17. Lanyi, J. K. (1993) *Biochim. Biophys. Acta* **1183,** 241–261
18. Wu, J., Sun, J., and Kaback, H. R. (1996) *Biochemistry* **35,** 5213–5219
19. Zani, M.-L., Pourcher, T., and Leblanc, G. (1993) *J. Biol. Chem.* **268,** 3216–3221
20. Keithly, J. S. (1976) *J. Protozool.* **23,** 244–245
21. Iovannisci, D. M., and Ullman, B. (1983) *Parasitology* **69,** 633–636
22. Langford, C. K., Little, B. M., Kavanaugh, M. P., and Landfear, S. M. (1994) *J. Biol. Chem.* **269,** 17939–17943
23. Hutchison, C. A., III, Swanstrom, R., Loeb, D. D. (1991) *Methods Enzymol.* **202,** 356–390
24. Titus, D. E. (1991) *Promega Protocols and Application Guide*, pp. 98–105, Promega Corp., Madison, WI
25. Viera, J., and Messing, J. (1987) *Methods Enzymol.* **153,** 3–11
26. Zell, R., and Fritz, H. J. (1987) *EMBO J.* **6,** 1809–1815
27. Sanger, F., Nicklen, S., and Coulson, A. R. (1977) *Proc. Natl. Acad. Sci. U. S. A.* **74,** 5463–5467
28. Arriza, J. L., Kavanaugh, M. P., Fairman, W. A., Wu, Y.-N., Murdoch, G. H., North, R. A., and Amara, S. G. (1993) *J. Biol. Chem.* **268,** 15329–15332
29. LeBowitz, J. H., Coburn, C. M., McMahon-Pratt, and Beverley, S. M. (1990) *Proc. Natl. Acad. Sci. U. S. A.* **87,** 9736–9740
30. Piper, R. C., Xu, X., Russell, D. G., Little, B. M., and Landfear, S. M. (1995) *J. Cell Biol.* **128,** 499–508
31. Zar, J. H. (1984) *Biostatistical Analysis*, pp. 150–153, Prentice-Hall, Englewood Cliffs, NJ
32. Lostao, M. P., Hirayama, B. A., Panayotova-Heiermann, M., Sampogna, S. L., Bok, D., and Wright, E. M. (1995) *FEBS Lett.* **377,** 181–184
33. Ballesteros, J. A., and Weinstein, H. (1995) *Methods Neurosci.* **25,** 366–428
34. Mancini, G. M. S., Beerens, C. E. M. T., and Verheijen, F. W. (1990) *J. Biol. Chem.* **265,** 12380–12387
35. Maiden, M. C. J., Davis, E. O., Baldwin, S. A., Moore, D. C. M., and Henderson, P. J. F. (1987) *Nature* **325,** 641–643
36. Pourcher, T., Zani, M.-L., and Leblanc, G. (1993) *J. Biol. Chem.* **268,** 3209–3215
37. Mueckler, M., Weng, W., and Kruse, M. (1994) *J. Biol. Chem.* **269,** 20533–20538
38. Gould, G. W., and Holman, G. D. (1993) *Biochem. J.* **295,** 329–341
39. Lachaal, M., Rampal, A. L., Lee, W., Shi, Y., Jung, C. Y. (1996) *J. Biol. Chem.* **271,** 5225–5230
40. Akabas, M. H., Stauffer, D. A., Xu, M., and Karlin, A. (1992) *Science* **258,** 307–310
41. Javitch, J. A., Fu, D., Chen, J., and Karlin, A. (1995) *Neuron* **14,** 825–831
42. Eisenberg, D., Schwarz, E., Komaromy, M., and Wall, R. (1984) *J. Mol. Biol.* **179,** 125–142

Aspartate 19 and Glutamate 121 Are Critical for Transport Function of the *myo* -Inositol/H^+ Symporter from*Leishmania donovani*

Andreas Seyfang, Michael P. Kavanaugh and Scott M. Landfear

J. Biol. Chem. 1997, 272:24210-24215.
doi: 10.1074/jbc.272.39.24210